Pergamon

Acta mater. Vol. 46, No. 11, pp. 3863–3872, 1998

Printed in Great Britain
PII: S1359-6454(98)00080-9
1359-6454/98 $19.00 + 0.00

CONTROL OF GRAIN GROWTH USING INTERGRANULAR SILICATE PHASES IN CUBIC YTTRIA STABILIZED ZIRCONIA

A. A. SHARIF[1], P. H. IMAMURA[1], T. E. MITCHELL[2] and M. L. MECARTNEY[1]†

[1]University of California, Irvine, Department of Chemical, Biochemical Engineering and Materials Science, Irvine, CA 92697-2575, U.S.A. and [2]Center for Materials Science, Los Alamos National Laboratory, Los Alamos, NM 87545, U.S.A.

(Received 9 October 1997; accepted 18 February 1998)

Abstract—Grain growth kinetics for 8 mol% yttria stabilized cubic zirconia (8Y–CSZ) were investigated. Optimal process parameters required to achieve a small grain size and full density for cubic 8Y–CSZ included a rapid heating rate (100°C/min) and hot isostatic pressing. Grain growth rates could also be controlled by the deliberate addition of 1 wt% of intergranular phases of borosilicate, barium silicate, and lithium aluminum silicate glasses. Lithium aluminum silicate, the intergranular phase with the highest solubility for yttria and zirconia, enhanced grain growth compared to control samples without grain boundary phases. The borosilicate intergranular phase, with the lowest solubility for yttria and zirconia, was the most effective in suppressing grain growth. Activation energies for grain growth were in the range of 400 kJ/mol, and the grain growth exponent ranged from 2 for lithium aluminum silicate containing samples, to 3 for pure samples, to 4 for barium silicate and borosilicate containing samples. © *1998 Acta Metallurgica Inc.*

1. INTRODUCTION

Much attention has recently been focused on the high temperature superplasticity which can be achieved in tetragonal yttria stabilized zirconia (Y–TZP), a tough ceramic used for structural applications [1–8]. Superplasticity is advantageous for easy and economical shape forming; however, the microstructural design of superplastic ceramics requires an ultrafine grain size that is stable against coarsening during sintering and deformation [4, 5]. Y–TZP ceramics have fine grain sizes ($< 1\ \mu$m) and abnormally sluggish grain growth rates during high temperature deformation; they are therefore perfect candidates for superplastic deformation. The slow grain growth is attributed to solute segregation and sluggish phase partitioning of the Y–TZP in the two-phase cubic–tetragonal region of the phase diagram [6].

Yttria stabilized cubic zirconia (Y–CSZ), is formed at higher concentrations of Y_2O_3 in solid solution [7]. Y–CSZ, with its high oxygen diffusion coefficient, has found application as a high performance solid electrolyte in high temperature electrochemical devices [9, 10]. Y–CSZ has large grain sizes ($> 10\ \mu$m) and high grain growth rates (30–250 times that of Y–TZP), more typical of conventional ceramics [11, 12]. A comparison of the dramatic difference in grain sizes for similarly processed 3 mol% Y_2O_3–TZP (3Y–TZP) and 8 mol% Y_2O_3–CSZ (8Y–CSZ) is shown in Fig. 1.

Due to the inherently large grain sizes and strain hardening caused by extensive dynamic grain growth during high temperature deformation, superplasticity has not been observed in Y–CSZ ceramics [2, 13, 14]. In order to achieve the high strain rates required for superplastic deformation of Y–CSZ ceramics, it would be necessary to limit intrinsic grain growth during sintering and prevent dynamic grain growth during deformation while promoting grain boundary sliding. The approach under investigation here is the addition of intergranular phases to 8Y–CSZ to limit grain growth as a first step to achieving superplasticity.

Intergranular phases in ceramics may originate from impurities in the raw materials or be introduced during processing as a sintering aid. The effects of grain boundary phases on the grain growth of yttria stabilized zirconia (YSZ) ceramics are not fully understood. Some investigators have reported grain growth enhancement due to the presence of a grain boundary phase in Y–TZP [15–17], others have found grain growth inhibition in the presence of an intergranular phase for Y–TZP [18], and some have reported a compositional dependence of the silicate grain boundary phases with respect to grain growth in Y–CSZ [19]. At the same

†To whom all correspondence should be addressed.

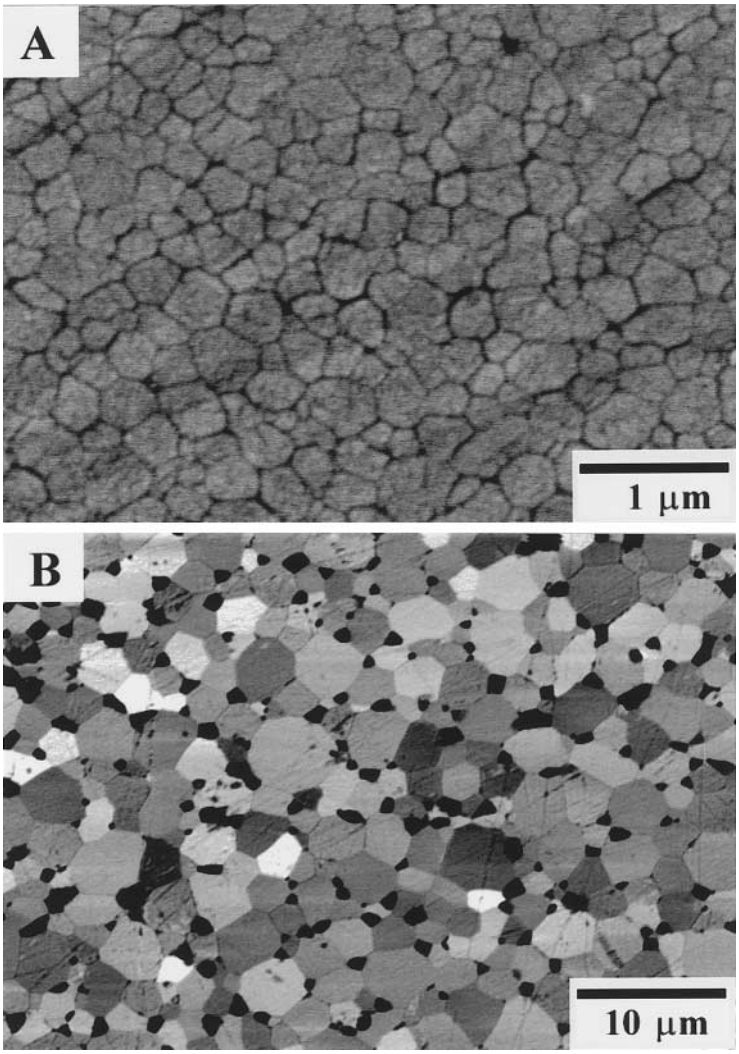

Fig. 1. An example of difference in grain sizes of (A) 3Y–TZP and (B) 8Y–CSZ both sintered at 1400°C in air for 2 h with a starting powder particle size of 20 nm. Note an order of magnitude difference in the scale bar.

time, certain glassy grain boundary phases have been shown to promote superplasticity in Y–TZP [8, 15, 17, 19–23]. The addition of small amounts, up to 3 vol.%, of silicate grain boundary phase has been shown to have little or no detrimental effect on the room temperature mechanical properties of Y–TZP [15].

Systematic studies of the effects of various intergranular phases on the rate of grain growth of CSZ have been lacking, a key omission since grain size control is a critical requirement for superplasticity. This current research investigates the use of inexpensive silicate grain boundary phases in 8Y–CSZ ceramics to limit grain growth in order to promote superplasticity. If successful, such a technique could be tailored to minimize grain growth and induce high temperature superplasticity in other ceramics by the addition of specific grain boundary phases.

2. EXPERIMENTAL PROCEDURE

Commercially available 8Y–CSZ powder (Tosoh, Japan) was used to prepare samples with no additives (hereafter called "pure samples") and samples with additives of 1 wt% barium silicate (BaS) (Specialty Glass, Florida), 1 wt% borosilicate (BS) (Specialty Glass, Florida), and 1 wt% lithium aluminum silicate (LiS) (Gwalia, Australia) glasses. Major constituents of these glasses are listed in Table 1. Powders of 8Y–CSZ and glass were made into a slurry by adding isoproponal. The slurry was stirred mechanically to obtain a uniform glass distribution then dried overnight at 120°C. The cake produced was crushed and the powder was sieved to $< 80\ \mu$m. The sieved powder was cold isostatically pressed at 400 MPa into cylinders of about 1 cm diameter and 1.2 cm height. Determination of

Table 1. Major constituents of three grain boundary phases selected for this study

Name	SiO_2	Al_2O_3	B_2O_3	Li_2O	Na_2O_3	K_2O	BaO	SrO	As_2O_3
BaS	45.8	2.1	21.6	—	—	—	29.2	0.7	0.5
BS	83.3	1.5	11.2	—	3.6	0.4	—	—	—
LiS	67.5	16.4	—	15.6	0.1	0.2	—	—	—

Values in mol%.

the optimum sintering temperature was accomplished by sintering samples of 8Y–CSZ at temperatures of 1200–1600°C for 0.1 h followed by hot isostatic pressing at 1400°C, 200 MPa for 0.25 h. Thereafter, all grain growth samples were first sintered at 1350°C for 0.1 h and hot isostatically pressed at 1400°C, 200 MPa for 0.25 h prior to annealing.

Seven coins were sectioned from each sample after hot isostatic pressing, polished down to 0.05 μm, ultrasonically cleaned in acetone and methanol, and placed in a rapid-heating box furnace for annealing up to 100 h in air at three temperatures of 1400, 1500, and 1600°C. For the grain growth experiments, each sample type was placed in an individual alumina crucible and covered with an alumina lid to prevent cross contamination. A heating rate of 100°C/min was used. Upon the expiration of the annealing time, the furnace was shut down and the samples were cooled to room temperature inside the furnace. The cooling rate was initially fast, about 100°C/min. Once the temperature reached below 1000°C, the cooling rate dropped to about 20°C/min. Samples were removed from the furnace after annealing times of 3, 10, 25, 50, 75, and 100 h. Scanning electron microscope (Philips XL 30 FEG) was used to obtain photomicrographs from thermally etched surfaces. The conventional mean linear intercept method was used on those photomicrographs to calculate the grain size. The reported grain size values are the average intercept length multiplied by 1.74 [24]. Sample density was determined by the use of Archimedes' method in distilled water. The solubility of yttria and zirconia in the intergranular phases was obtained by analytical transmission electron microscopy using a 300 keV Philips CM30 equipped with energy dispersive spectroscopy (EDAX).

3. RESULTS

3.1. Determination of optimal process conditions

The effect of sintering temperature and heating rate on microstructural development was studied first. It was found that for the same sintering time and temperature, a heating rate of 100°C/min resulted in a grain size of 8 μm vs a grain size of 14 μm if a conventional heating rate of 10°C/min was employed. Using a fast heating rate but decreasing the sintering time from 2 to 0.1 h resulted in a finer grain size of 2.5 μm, but a significant amount of residual porosity remained (only 93% dense). This combination of fast heating rates and short sintering times created a finer grain microstructure but in order to obtain full density, samples were hot isostatically pressed after sintering at various temperatures.

Analysis of the sample densities and grain sizes for pure samples after hot isostatic pressing at 1400°C showed that only samples pre-sintered at temperatures of 1350 and 1400°C had nearly full densities and relatively small grain sizes (Fig. 2). The decrease in density at higher sintering temperatures was unexpected but this effect could be due to the rapid heating rate (100°C/min) generating a high degree of trapped porosity in the grains due to rapid grain growth. Lower sintering temperatures would allow grain boundary pores to shrink via vacancy diffusion along the grain boundaries to the surface prior to grain growth. Hence, the two-step process of pre-sintering at 1350°C for 0.1 h with a heating rate of 100°C/min followed by hot isostatic pressing at 1400°C for 0.25 h gave optimum results of small grain sizes and high densities.

All the samples were sintered at 1350°C for 0.1 h and hot isostatically pressed at 1400°C, 200 MPa for 0.25 h prior to annealing for the grain growth studies. The sinter/hot isostatic pressing process resulted in small grain sizes (about 3 μm) and almost full density for all samples except those containing BaS (Table 2). Figures 3(a)–(d) show the microstructures of samples of 8Y–CSZ with various grain boundary phases after sintering and hot isostatic pressing but prior to annealing. Pre-sintered samples containing BaS had relatively low densities, $<85\%$ theoretical; hence, the presence of open porosity prevented their densification during hot isostatic pressing. Large pores attached to grain boundaries can be seen in the BaS samples [Fig. 3(b)]. A nonuniform distribution of the intergranular phase was initially present in some regions of BS and LiS samples [Figs 3(c) and (d)].

3.2. Annealing

Representative micrographs of sample microstructures with different intergranular phases after annealing 100 h at 1400°C in air are shown in Fig. 4. The pure sample of 8Y–CSZ has a faceted equiaxed grain morphology with sharp multiple grain junctions [Fig. 4(a)]. Samples containing BaS grain boundary phase [Fig. 4(b)] have a smaller grain size (9 μm) than the pure samples (12 μm). The BaS samples had a relatively low density (83% theoretical) prior to annealing; however, these

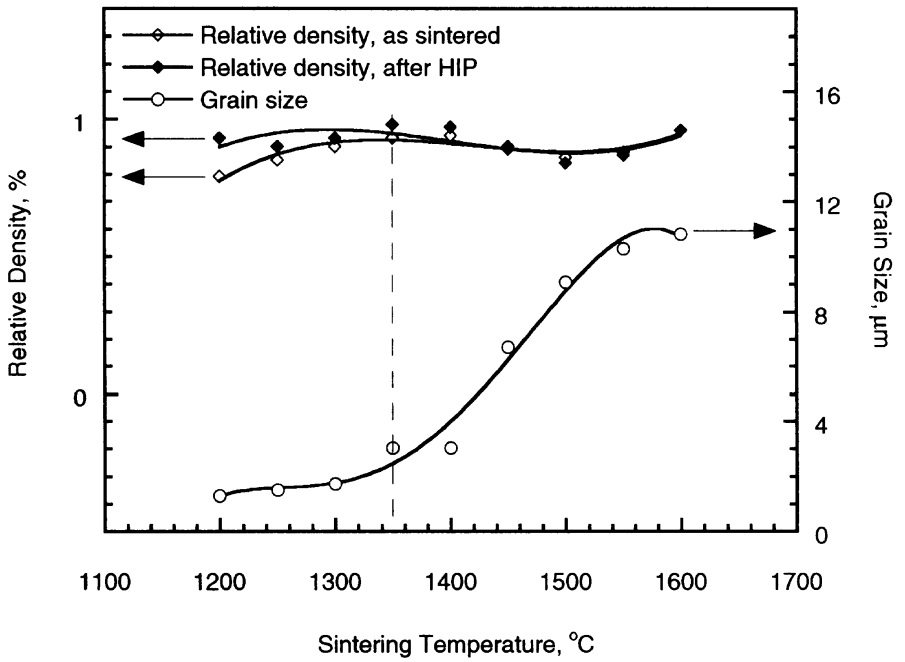

Fig. 2. Effect of sintering temperature (0.1 h sintering time) and HIP (0.25 h hold time) on density and grain size of 8Y–CSZ.

samples increased to 90% relative density during long annealing times. A fairly uniform grain size distribution with many equiaxed grains and highly etched grain boundaries is observed in these samples. In BS containing samples [Fig. 4(c)], the glass phase is less uniformly distributed. In regions adjacent to the glass phase, the grains are smaller than those areas void of glassy phase. Hence, a dual grain size distribution was observed in these samples ($d_1 = 4\ \mu$m, $d_2 = 12\ \mu$m after 100 h at 1400°C). LiS containing samples have the largest grain size among all the samples (16 μm after 100 h at 1400°C). A continuous uniform grain boundary layer appears to be present in these samples [Fig. 4(d)].

At high temperatures and long times, abnormal grain growth was observed in pure samples sintered without a hot isostatic pressing step. Abnormal grain growth was never observed in glass-containing samples.

A representative plot of the grain size vs time for all samples at the highest annealing temperature of 1600°C is shown in Fig. 5. The slowest grain growth was observed in samples containing BS glass and the fastest grain growth rate occurred in samples with LiS glass.

3.3. Grain growth

The kinetics of grain growth were studied by the use of the phenomenological grain growth equation [25]

$$D^n - D_0^n = Kt$$

$$K = K_0 \exp\left(\frac{-Q}{RT}\right)$$

where D is the instantaneous grain size at time t, D_0 the grain size at $t = 0$, n the grain growth exponent, K a kinetic constant which depends on temperature and grain boundary energy, K_0 a temperature insensitive constant, and Q, R, T are activation energy, gas constant, and absolute temperature, respectively. The grain growth exponent, n, is obtained by plotting $\ln D$ vs $\ln t$ as shown in Figs 6(a)–(d). The slope of the straight line obtained from such a plot is the inverse of the grain growth exponent, $1/n$. The activation energy, Q, for

Table 2. Sample grain sizes and densities before and after hot pressing

	Sintered at 1350°C, 0.1 h		After HIP at 1400°C, 0.25 h	
Sample	Grain size (μm)	Relative density (%)	Grain size (μm)	Relative density (%)
8–YSZ	2.5	93	3.5	100
8–YSZ + 1 wt% BaS	2.5	80	3.4	83
8–YSZ + 1 wt% BS	2.4	97	3.2	99
8–YSZ + 1 wt% LiS	3.0	93	4.6	100

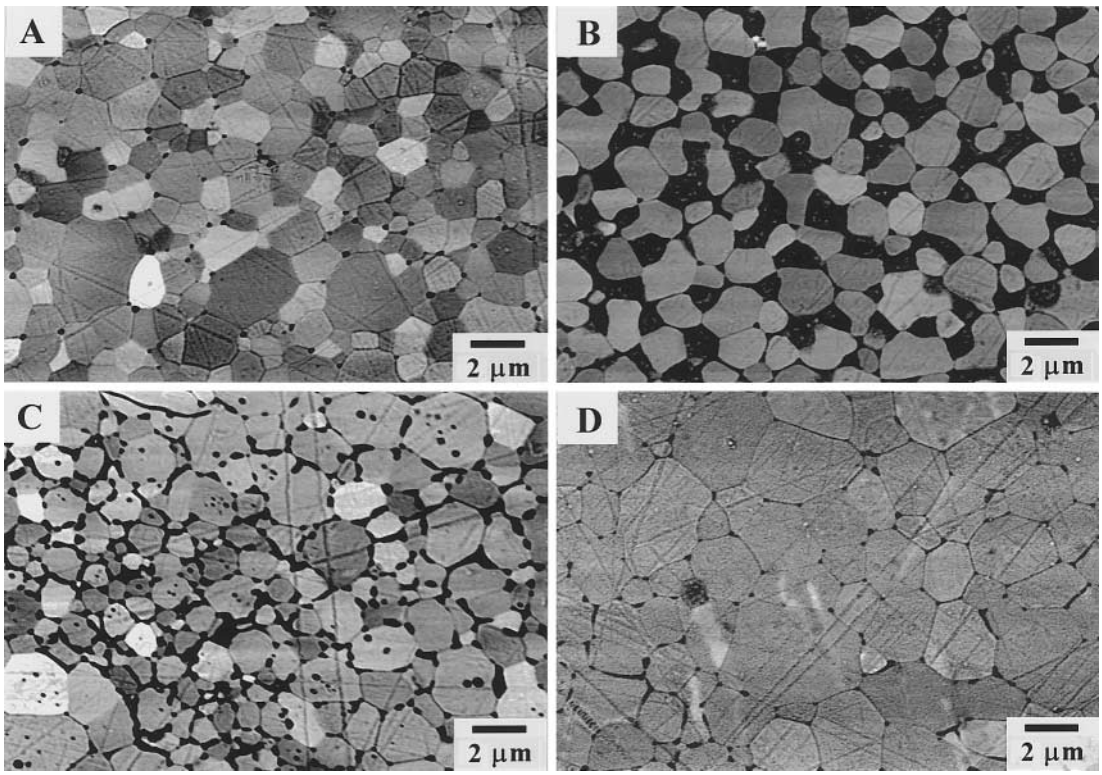

Fig. 3. Starting grain sizes of samples of 8Y–CSZ with various grain boundary phases prior to annealing (sintered 0.1 h at 1350°C, heating rate of 100°C/min, HIP at 1400°C, 200 MPa for 0.25 h): (A) pure 8Y–CSZ; (B) 8Y–CSZ + 1 wt% BaS; (C) 8Y–CSZ + 1 wt% BS; (D) 8Y–CSZ + 1 wt% LiS.

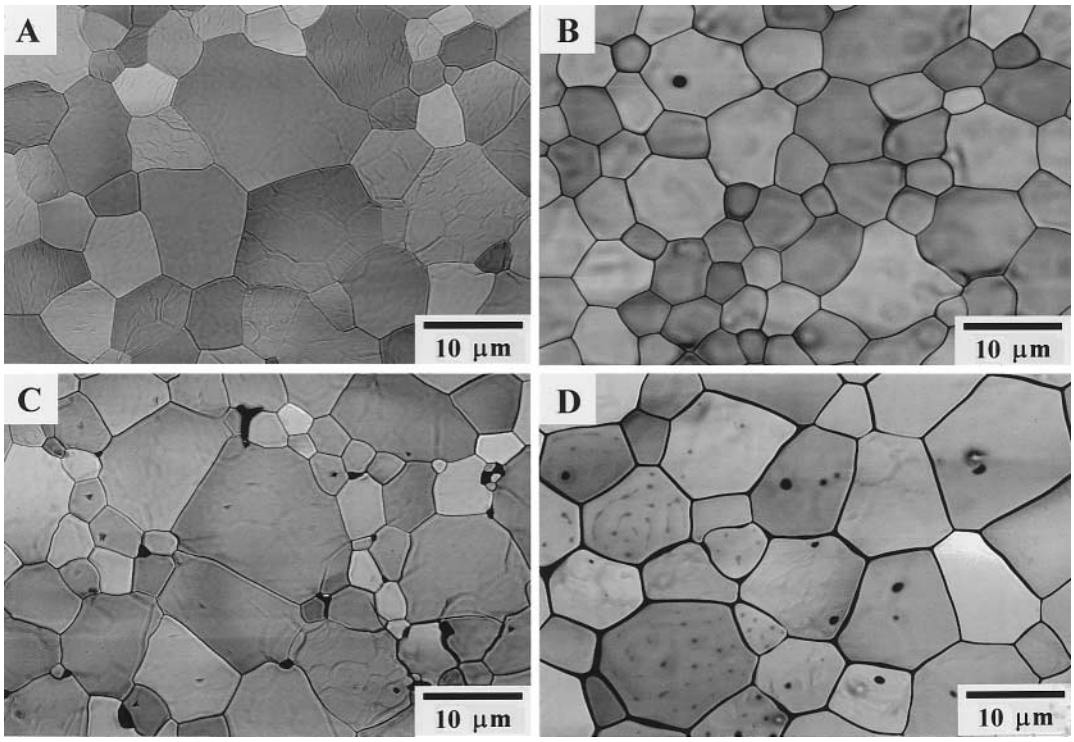

Fig. 4. SEM micrographs of samples after 100 h anneal at 1400°C: (A) pure 8Y–CSZ; (B) 8Y–CSZ + 1 wt% BaS; (C) 8Y–CSZ + 1 wt% BS; (D) 8Y–CSZ + 1 wt% LiS.

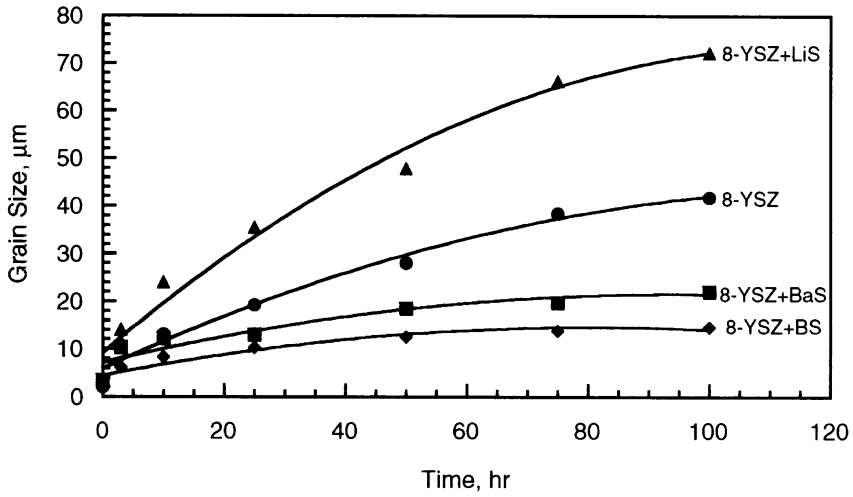

Fig. 5. Grain size as a function of time for samples annealed at 1600°C.

the grain growth is calculated from the slope of the line obtained from the plot of $\ln((D^n - D_0^n)/t)$ vs $1/T$ as shown in Fig. 7.

4. DISCUSSION

A fairly uniform grain size distribution was observed in pure samples of 8Y–CSZ [Fig. 4(a)]. The smallest grain sizes were obtained in samples with BS glass [Fig. 4(c)], and the only intergranular phase which resulted in a faster growth rate than pure samples was that in the LiS containing samples (Fig. 5). The BS and LiS grain boundary phases have the lowest and highest solubilities for ZrO_2 and Y_2O_3, respectively (Table 3). The higher solubility intergranular phases have a more open/broken network due to the presence of network modifiers Ba^{2+} and Li^+ ions. The highest solubility intergranular phases would have the lowest viscosity at high temperatures and highest diffusivity. BS contains B^{3+} ions, a network former; it is known to have a high viscosity and is expected to have low diffusivity. The addition of BS to the system will result in limiting the matter transfer via the grain boundary resulting in slower grain growth. Figure 4(c) shows that the BS intergranular phase is effective in pinning the grain boundary and limiting grain growth. Its higher viscosity did not permit a

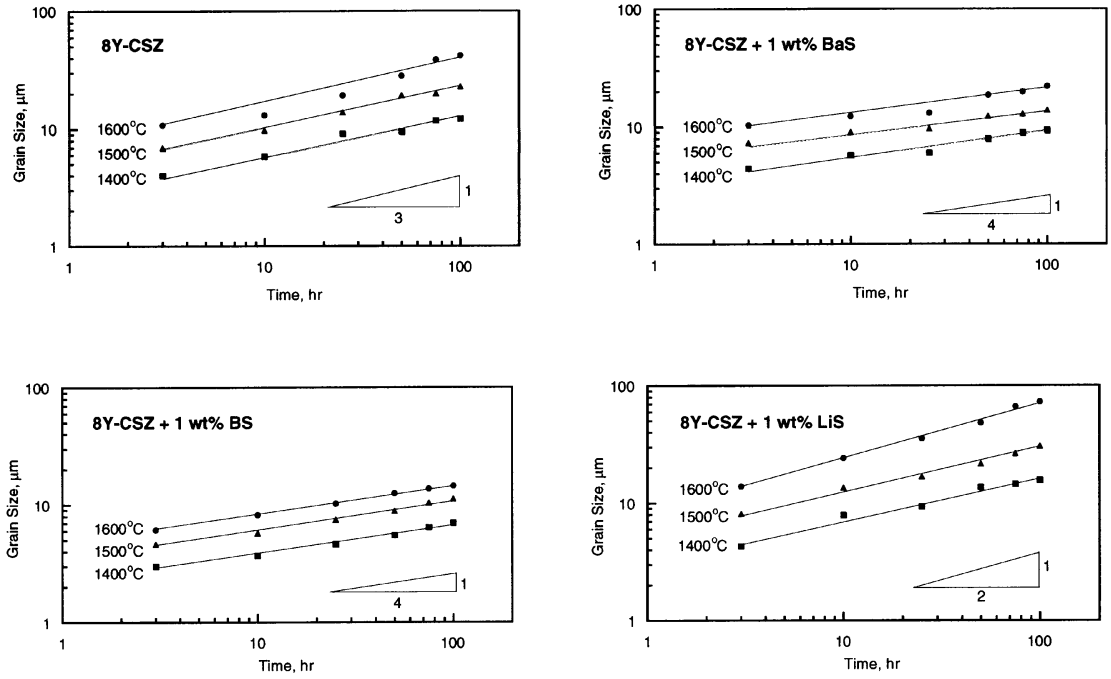

Fig. 6. Grain size vs time ln–ln plots for temperatures from 1400 to 1600°C. The inverse of the slope is the grain growth exponent, n.

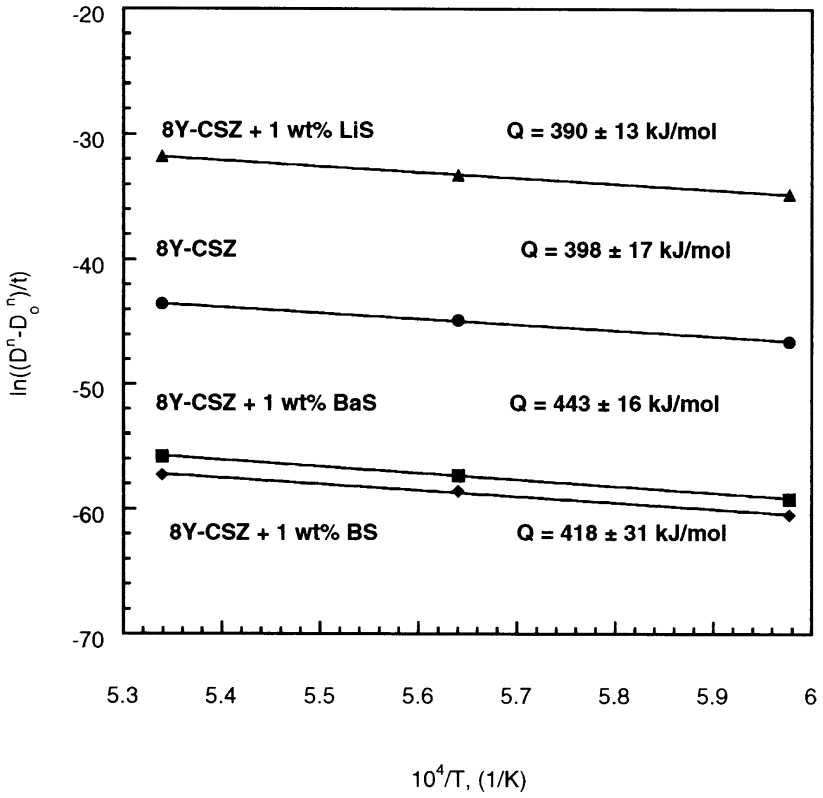

Fig. 7. Arrhenius plots for all four sample compositions. The slope is the activation energy for grain growth.

uniform distribution of the intergranular phase for short times and low temperatures.

If the effect of glassy intergranular phases on grain growth of Y–CSZ could be simply predicted by the relative solubilities of the glass for ZrO_2 and Y_2O_3, similarly fast grain growth behavior would be expected for BaS and LiS samples due to their high solubilities for ZrO_2 and Y_2O_3 (Table 3). The sluggish grain growth in BaS samples relative to LiS samples can be explained as a result of suppressed sintering due to the presence of the BaS glass. Incomplete sintering leaves the samples with high residual porosity. The high amount of residual porosity initially present in BaS samples [Fig. 3(b)] would act as a pinning agent for the grains and hinder grain growth. Two growth regions may be distinguished in the BaS samples, a slow growth region occurring up to 25 h and a fast growth region after 25 h of annealing. These regions may be distinguished by a break that can be seen at 25 h in the $\ln t$ vs $\ln D$ plot in Fig. 6(b) ($\ln 25 = 3.2$).

Table 3. Solubilities of zirconia and yttria in grain boundary phases

Phase	ZrO_2 (%)	Y_2O_3 (%)
Spodumene (LiS)	31	7
Barium silicate (BaS)	21	7
Borosilicate (BS)	4	1

Values in mol%.

After 25 h annealing at all temperatures, the samples attain higher density and the pinning effect of extensive porosity is not present.

Another effect on grain growth that can be attributed to the presence of the grain boundary phases is the absence of abnormal grain growth in any sample containing a grain boundary phase. Abnormal grain growth was observed during annealing above 1500°C only in pure samples which were not hot isostatically pressed. The presence of a grain boundary phase effectively eliminates the possibility of attaining intrinsic grain growth rates; of course, some solute drag effect will always be present even in nominally "pure" samples since the grain boundaries are not perfectly clean. At high temperatures the driving force for grain growth can be large enough in "pure" samples to overcome the solute drag effect. In addition, for longer times at high temperatures impurity solute atoms at the grain boundaries may be dissolved into the zirconia minimizing the solute drag effect. Hence, the presence of abnormal grain growth is most likely an indication that the true intrinsic grain growth rate for the material is being approached. The reason for the suppression of abnormal grain growth in hot pressed samples is not fully understood. It is believed that some contamination introduced during the hot isostatic pressing process is responsible for creating a higher amount of solute drag in these

Table 4. Values of kinetics constants for grain growth of YSZ reported by various authors

Author	Material	Grain growth exponent	Activation energy (kJ/mol)
Present work	8Y–CSZ	3	398 ± 17
Present work	8Y–CSZ + BaS	4	443 ± 16
Present work	8Y–CSZ + BS	4	418 ± 31
Present work	8Y–CSZ + LiS	2	390 ± 13
Yoshizawa and Sakuma [12]	8Y–CSZ	2	—
Lee and Chen [11]	8Y–CSZ	2	289
Lee and Chen [11]	2Y–TZP	2	440
Nieh *et al.* [5]	Y–TZP	3	580

samples and may limit these pure samples from achieving intrinsic grain growth.

The value of the grain growth exponent, n, calculated from Fig. 6, is expected to depend on the sample microstructure [26]. This value may vary between 1 and 4 depending on the rate limiting step during grain boundary migration [25]. The best fit values of n obtained during these studies were approximately 3 for pure samples, 4 for BaS and BS containing samples, and 2 for LiS containing samples.

Normal grain growth is predicted to follow a parabolic relation, hence, $n = 2$. The parabolic growth law is usually exhibited only in pure single-phase systems at high temperatures [25]. The value of 3 for n for pure 8Y–CSZ samples possibly indicates grain growth controlled by impurity drag. In an ionic solid such as 8Y–CSZ, the boundary velocity due to impurity drag control growth would be affected by the concentration of the impurity and the effect of introduced point defects on the rate of diffusion [25]. The value of $n = 3$ has also been observed for grain growth in Y–TZP samples [5]. The value of $n = 4$ for BaS samples reflects the higher porosity in samples with BaS glass. The relatively slow grain growth observed in BaS samples probably is due to the control of boundary motion by pore migration involving surface diffusion of atoms which will give an n value of 4 [25]. However, the same mechanism should not be valid for the n value of 4 in BS containing samples since these samples had nearly full density. In this case, a mechanism of grain boundary diffusion which also produces an n value of 4 is believed to control the growth rate of BS samples [25]. The value of 2 for n for LiS samples could be representative of an interface reaction controlled grain growth in the presence of a continuous liquid phase since the SEM analysis of the LiS containing samples in Fig. 4(d) suggests that a continuous grain boundary phase may be present [27].

A range of values for n has been reported by various investigators for grain growth of YSZ ceramics (Table 4). Lee and Chen [11], and Yoshizawa and Sakuma [12] studied the grain growth of nominally pure 8Y–CSZ. Both groups of investigators found that their data fit best to a parabolic rate law with a grain growth exponent of 2. The different grain growth exponents calculated for these samples of varying intergranular compositions indicate the presence of different grain growth mechanisms for various samples as discussed above. However, the value of the activation energies for grain growth for all samples in the current study were similar, ranging from 390 to 443 kJ/mol (Fig. 7). The value of 398 kJ/mol for the activation energy for the grain growth of pure 8Y–CSZ is much lower than the activation energy of 580 kJ/mol reported by Nieh *et al.* [5] for grain growth of Y–TZP, an expected result since grain growth in Y–TZP is much more sluggish than that in 8Y–CSZ. Lee and Chen [11] calculated the activation energy for the grain growth of 2Y–TZP to be 440 kJ/mol and for 8Y–CSZ to be only 289 kJ/mol at 1300–1700°C using $n = 2$ for both materials (Table 4). They attributed the fast growth rate in the cubic phase to higher mobility of the grain boundary of the cubic grains than the tetragonal grains. The calculation of the activation energy depends sensitively on the best fit value of n selected and if a value of $n = 2$ had been chosen, the activation energy for pure 8Y–CSZ would be 270 kJ/mol, in the same range as Lee and Chen's data for 8Y–CSZ.

A higher value of activation energy was expected for grain growth of BS containing samples since the grain growth was sluggish in comparison to pure or LiS samples. There are two possible explanations for the unexpected lower activation energy calculated here for BS containing samples. First, the nonuniform grain size distribution due to the nonuniform distribution of the intergranular phase in these samples may have contributed to the introduction of an error in determining accurate grain sizes during analysis. Second, the energy associated with entropy may not be negligible in BS containing samples due to the nonuniform mixing. In the derivation of the phenomenological grain growth equation from the Gibbs free energy equation ($G = \Delta H - T\Delta S$), the entropy term ($-T\Delta S$) is assumed to be negligible compared to the enthalpy term (ΔH) [25]. The slope of the line obtained by plotting $\ln(D^n)$ vs $1/T$ measures the activation enthalpy (ΔH) rather than the activation free energy for grain growth and ignores the entropy contribution [28]. At high temperatures, even small values of the entropy of mixing may render the term ($-T\Delta S$) a non-negligible contribution to the free energy. A better distribution of the low solubi-

lity intergranular phase would be more effective in generating a more uniformly fine grain size microstructure and would minimize the problem.

The cubic 8Y–CSZ materials discussed in this paper do have an initial grain size (3 μm) which is an order of magnitude larger than the grain size of tetragonal Y–TZP (0.3 μm) used for superplastic deformation and three times larger than the expected critical (maximum) grain size (1 μm) for structural superplasticity in fine-grained ceramics [29]. However Tsurui and Sakuma [30] have found that the addition of 5 wt% TiO_2 to 2.5Y–TZP resulted in a decrease in superplastic flow stress, although the grain size increased to 2.6 μm. Hence, the critical grain size for superplasticity in ceramics may be increased with the addition of secondary phases.

Preliminary research on BS containing 8Y–CSZ samples with a fairly uniform distribution of the intergranular phase showed enhanced high temperature deformation and minimal grain growth. This material was deformed uniformly to 40% strain under compression at 1400°C. The strain rate was 8.3×10^{-6}/s with applied stress of 15 MPa for samples containing 1 wt% BS. In comparison, the strain rate was 4×10^{-8}/s with a higher applied stress of 50 MPa for pure 8Y–CSZ. Although these initial experiments do not show superplastic deformation for 8Y–CSZ with an intergranular phase, an increase in the amount of intergranular phase or modifications of the intergranular composition may further enhance the deformation. The presence of a viscous intergranular phase may promote superplastic deformation at temperatures lower than those expected for these grain sizes.

Recent research on the addition of high viscosity SiO_2 to Y–TZP indicates that although the superplastic flow stress is higher than when using lower viscosity intergranular phases, tensile elongations over 1000% can be achieved for pure Y–TZP [8]. High viscosity, low diffusivity intergranular phases may inhibit dynamic grain growth while promoting grain boundary sliding and allowing these extensive elongations.

5. SUMMARY

Relatively small grain sizes of approximately 3 μm and densities of 99% theoretical were obtained for 8Y–CSZ by using a two-step rapid heating sinter/hot isostatic pressing fabrication process. Silicate intergranular phases inhibited abnormal grain growth. A grain growth exponent of 3 and activation energy for grain growth of 398 kJ/mol were obtained for pure 8Y–CSZ. The presence of a high solubility lithium–aluminum–silicate grain boundary phase in the sample resulted in faster grain growth than for pure 8Y–CSZ with a grain growth exponent of 2 and activation energy for grain growth of 390 kJ/mol. Two other glasses, namely barium silicate and borosilicate, were found whose addition to the 8Y–CSZ resulted in grain growth inhibition. The barium silicate containing samples had a grain growth exponent of 4 and activation energy for grain growth of 443 kJ/mol, but grain growth appeared to be limited by residual porosity. The most effective intergranular phase for limiting grain growth was the low solubility borosilicate phase with a grain growth exponent of 4 and an activation energy for grain growth of 418 kJ/mol. Small addition of low solubility intergranular phases may be a highly effective route to producing fine grain ceramics, a first step to superplasticity.

Acknowledgements—The ideas forming the basis of this work were developed initially with support from a Davis and Lucille Packard Fellowship in Science and Engineering (MLM). Support for the experimental portion of the research was provided by a grant from the Collaborative UC/Los Alamos Research program. The purchase of the field emission scanning electron microscope was made possible through instrumentation grant DMR 9503774 from the NSF.

REFERENCES

1. Subbaro, E. C., in *Science and Technology of Zirconia*, ed. A. H. Heuer and L. W. Hobbs, Vol. 3. The American Ceramic Society, Inc., Columbus, Ohio, 1980, p. 1.
2. Wakai, F., Sakaguchi, S. and Matsuno, Y., *Adv. Ceram. Mater.*, 1986, **1**, 259.
3. Garvie, R. C., Hannink, R. H. and Pascoe, R. T., *Nature*, 1975, **258**, 703.
4. Chen, I.-W. and Xue, L. A., *J. Am. Ceram. Soc.*, 1990, **73**, 2585.
5. Nieh, T. G., Tomasello, C. M. and Wadsworth, J., in *Superplasticity in Metals, Ceramics, and Intermetallics*, Vol. 196, ed. M. J. Mayo, M. Kobayashi and J. Wadsworth. MRS, San Francisco, California, 1990, p. 343.
6. Lange, F. F., *J. Am. Ceram. Soc.*, 1986, **69**, 240.
7. Brook, R. J., in *Science and Technology of Zirconia*, Vol. 3, ed. A. H. Heuer and L. W. Hobbs. The American Ceramic Society, Inc., Columbus, Ohio, 1980, p. 272.
8. Sakuma, T. and Yoshizawa, Y.-I., *Materials Science Forum*, 1994, **170–172**, 369.
9. Hagenmuller, P. and Gool, W. v., *Solid Electrolytes*. Academic Press, New York, 1978.
10. Aoki, M.*et al.*, *J. Am. Ceram. Soc.*, 1996, **79**, 1169.
11. Lee, I. G. and Chen, I.-W., in *Sintering 87*, Vol. 1, ed. S. Somiya, M. Yoshimura and R. Watanabe. Elsevier, London, 1988, p. 340.
12. Yoshizawa, Y. I. and Sakuma, T., *ISIJ Int.*, 1989, **29**, 746.
13. Nieh, T. G., McNally, C. M. and Wadsworth, J., *Scripta metall.*, 1988, **22**, 1297.
14. Nieh, T. G. and Wadsworth, J., *J. Am. Ceram. Soc.*, 1989, **72**, 1469.
15. Gust, M., Goo, G., Wolfenstine, J. and Mecartney, M. L., *J. Am. Ceram. Soc.*, 1993, **76**, 1681.
16. Hwang, C. M. J. and Chen, I. W., *J. Am. Ceram. Soc.*, 1990, **73**, 1626.
17. Yoshizawa, Y.-i. and Sakuma, T., *J. Am. Ceram. Soc.*, 1990, **73**, 3069.
18. Schubert, H., Claussen, N. and Rühle, M., in *Advances in Ceramics*, Vol. 12, *Science and Technology of Zirconia II*, ed. N. Claussen, M. Rühle and A. H.

Heuer. The American Ceramic Society, Inc., Columbus, Ohio, 1984, p. 766.
19. Lin, Y.-J., Angelini, P. and Mecartney, M. L., *J. Am. Ceram. Soc.*, 1990, **73**, 2728.
20. Wakai, F., Kondo, N., Ogawa, H., Nagano, T. and Tsurekawa, S., *Materials Science Forum*, 1997, **243–245**, 337.
21. Yoshizawa, Y.-I. and Sakuma, T., in *Proc. 1st Japan International SAMPE Symposium*, 1989, 272 pp.
22. Chaim, R. and Heuer, A. H., *J. Am. Ceram. Soc.*, 1986, **69**, 243.
23. Kajihara, K., Yoshizawa, Y. and Sakuma, T., *Acta metall. mater.*, 1995, **43**, 1235.
24. Thompson, A. W., *Metallography*, 1972, **5**, 366.
25. Brook, R. J., in *Treatise on Materials Science and Technology*, Vol. 9. Academic Press, New York, 1976, p. 331.
26. Allemann, J. A., Michel, B., Märki, H.-B., Gauckler, L. J. and Moser, E. M., *J. Eur. Ceram. Soc.*, 1995, **15**, 951.
27. Bennison, S. J., in *Ceramics and Glasses*, Vol. 4, ed. T. J. Reinhart. ASM International, Metals Park, Ohio, 1987, p. 304.
28. Shi, F. G., *Scripta metall. mater.*, 1994, **31**, 1227.
29. Maehara, Y. and Langdon, T. G., *J. Mater. Sci.*, 1990, **25**, 2275.
30. Tsurui, K. and Sakuma, T., *Scripta mater.*, 1996, **34**, 443.